Journal of Materials Science: Materials in Electronics (2020) 31:3835–3844
https://doi.org/10.1007/s10854-020-02918-6

Structure, energy transfer, and luminescence properties of $NaLaMgWO_6$: Tb^{3+},Eu^{3+} phosphors for solid-state lighting

Guifang Li[1] · Yu Wang[1] · Yunge Wei[1] · Xiaohui Wang[1]

Received: 10 September 2019 / Accepted: 16 January 2020 / Published online: 3 February 2020

Abstract
Novel $NaLaMgWO_6$:Tb^{3+},Eu^{3+} phosphors with tunable color emissions were prepared by a solid-state reaction. The crystal structure, composition, and luminescent properties of the obtained phosphors were investigated by X-ray diffraction (XRD), scanning electron microscope (SEM), and fluorescence spectrophotometer. The results reveal that $NaLaMgWO_6$ crystallizes in a monoclinic double perovskite structure with *C*2/*m* space group. Tb^{3+} and Eu^{3+} single-doped phosphors show the intense green and red emissions at 545 and 617 nm, corresponding to the $^5D_4 \rightarrow {}^7F_5$ transition of Tb^{3+} and the $^5D_0 \rightarrow {}^7F_2$ transition of Eu^{3+}, respectively, while for Tb^{3+} and Eu^{3+} co-doped phosphors, a tunable emission color from green to red is obtained by variation of the ratio of Eu^{3+} to Tb^{3+}. The emission spectra and luminescence decay lifetimes verify the occurrence of energy transfer from Tb^{3+} to Eu^{3+} in $NaLaMgWO_6$: Tb^{3+}, Eu^{3+} phosphor, and the energy transfer mechanism is dominated by the dipole–quadrupole interaction. Furthermore, the thermal stability of $NaLaMgWO_6$:Tb^{3+}, Eu^{3+} phosphor was discussed from 305 to 515 K. The results exhibit the phosphors possess excellent thermal stability, and the activation energy is calculated to be 0.302 eV.

1 Introduction

Phosphor-converted white light emitting diodes (pc-LEDs) have been used in numerous fields, such as indoor and outdoor lighting, screen display, and safety warning, because of their environmental friendliness, long lifetime, high brightness, and reliability. Nowadays, the most common way to achieve white LEDs is to combine a blue LED chip (InGaN) with yellow-emitting phosphors ($Y_3Al_5O_{12}$:Ce^{3+}) [1, 2]. However, the deficiency of red-emitting component leads to poor color-rendering index and low stability of color temperature that restrict its applications. To circumvent these drawbacks, ultraviolet (UV) LED chips can be combined with tricolor (blue, green, and red) phosphors to obtain high-quality white LEDs. Nevertheless, they still suffer from some problems, such as low luminous efficiency and poor color stability because of the strong reabsorption of blue light by the red and green phosphors. Using single-phase phosphors with tunable emission can effectively avoid the above problems [3, 4]. Therefore, it is important and urgent to explore single-phase tunable color phosphors with high luminescent efficiency under UV.

On the basis of energy transfer from the sensitizer to the activator, the combination of multiple activator ions in single-phase host is assumed to be a feasible method to realize tunable color emission [5]. In the rare earth family, the Eu^{3+} and Tb^{3+} ions are well considered as a promising red and green emitting activator for their characteristic $^5D_0 \rightarrow {}^7F_2$ transition and $^5D_4 \rightarrow {}^7F_5$ transitions, respectively. Meanwhile, when Tb^{3+} and Eu^{3+} ions are co-doped in a single-phase host, Tb^{3+} ion as a good sensitizer can transfer its energy to activator Eu^{3+} with the phonon spectrum. By adjusting the Eu^{3+}/Tb^{3+} ratio, color-tunable emission can be realized in Tb^{3+} and Eu^{3+} co-doped phosphors [6, 7]. Consequently, plenty of researches on Tb^{3+} and Eu^{3+} ion co-doped phosphors have been proposed to obtain abundant emitting colors, such as $CaGd_2(WO_4)_4$:Tb^{3+}, Eu^{3+} [6], $KBaGd(WO_4)_3$:Tb^{3+}, Eu^{3+} [7], $Sr_3La(PO_4)_3$:Tb^{3+}, Eu^{3+} [8], and Na_2MgSiO_4:Tb^{3+}, Eu^{3+} [9]. In general, the luminescence properties of rare earth ions (Tb^{3+} and Eu^{3+}) depend on the host crystal structure, so it is important to select an appropriate host to obtain efficient phosphors. Recently, double perovskite structure compounds with the general formula AA'BB'O_6 (where A = K, Na, Li; A' = Gd, La; B = Ca, Mg; B' = W, Mo) being host doped with a variety of

✉ Guifang Li
gfli@mail.xidian.edu.cn

[1] School of Advanced Materials and Nano Technology, Xidian University, Xi'an 710071, China

activators have been studied extensively due to their excellent luminescence characteristics and chemical and physical properties [10–13]. AA'BB'O_6 compound exhibits the diversity of crystal structure with the different ion types of A/A' and B/B'. Among them, the representative compound $NaLaMgWO_6$ possesses a monoclinic structure with the space group of *C*2/*m*. It has double ordering structural characteristics: the layered A site cation ordering (Na^+/La^{3+}) and rock salt B site cation ordering (Mg^{2+}/W^{6+}) [14]. The structure provides lots of crystal field to co-dope numerous rare earth ions, which is beneficial to tune the luminescent characteristics. Furthermore, $NaLaMgWO_6$ host shows broad and strong charge transfer band in the UV, and the energy could effectively transfer to rare earth activators, resulting in the enhancement of luminous efficiency. As a result, rare earth ion-doping $NaLaMgWO_6$ phosphors have been widely studied, especially Eu^{3+} single-doped $NaLaMgWO_6$:Eu^{3+} red-emitting phosphors, as the suitable candidate for high-performance white LEDs [13–16]. However, no report is available on the luminescence properties and the energy transfer between Tb^{3+} and Eu^{3+} in $NaLaMgWO_6$:Tb^{3+}, Eu^{3+} phosphors.

In this paper, a series of Tb^{3+} and Eu^{3+} co-doped $NaLaMgWO_6$ phosphors were prepared by the solid-state reaction technique and their crystal structure, photoluminescence properties, and thermal stability were systematically discussed. Under excitation at 273 nm, $NaLaMgWO_6$:Tb^{3+}, Eu^{3+} phosphors generate tunable color emission from green to red by tuning the ratio of Eu^{3+} to Tb^{3+}. Evidence of energy transfer from Tb^{3+} to Eu^{3+} was illustrated via the emission spectrum and decay curve measurements.

2 Experimental section

The phosphor samples $NaLa_{1-x-y}MgWO_6$:xTb^{3+},yEu^{3+} ($0 \le x \le 0.15$; $0 \le y \le 0.8$) were prepared via the high-temperature solid-state technique. Firstly, stoichiometric amounts of raw materials Na_2CO_3 (A.R), $MgCO_3$ (A.R), La_2O_3 (99.95%), Eu_2O_3 (99.9%), Tb_4O_7 (99.9%) and WO_3 (99.9%) were weighed and mixed thoroughly in a planetary ball mill. The ball-milled mixtures were put into a Petri dish and dried in a drying oven at 80 °C. Then, the homogeneous powders were calcined at 1100 °C for 4 h and cooled to room temperature with the furnace. Finally, the obtained samples were ground again for further characterizations.

The X-ray diffraction (XRD) patterns of the phosphors were collected using an X-ray diffractometer (D8 Advance, Bruker, Germany) with Cu K_α ($\lambda = 0.15418$ nm) radiation at 40 kV and 40 mA. The morphology and composition analysis of the samples were obtained via a field emission scanning electron microscopy (Apreo + HiVac, FEI, America) equipped with energy-dispersive spectrometer (EDS). The photoluminescence spectra were characterized using a fluorescent spectrometer (F-7000, Hitachi, Japan), and TAP-02 high-temperature fluorescent controller was equipped to the spectrometer to measure the temperature-dependent emission spectra. The fluorescence decay curves were collected with a FluoroLog-3 fluorescence spectrophotometer (Jobin–Yvon, Horiba, France).

3 Results and discussion

3.1 Phase analysis

Figure 1 shows the XRD patterns of $NaLa_{0.9-y}MgWO_6$:$0.1Tb^{3+}$, yEu^{3+} ($0 \le x \le 0.8$) phosphors. It is clearly seen that all the diffraction peaks are consistent with (NaLa)(MgW)O_6 standard diffraction card (JCPDS 37-0243). This result indicates that all studied phosphors have the same monoclinic double perovskite structure without any other impurity phase. In other words, Tb^{3+} and Eu^{3+} have been successfully incorporated into the host lattice without any structural changes. Furthermore, as shown in Fig. 1b, as the Eu^{3+} doping concentration increases, the diffraction peaks of $NaLa_{0.9-y}MgWO_6$:$0.1Tb^{3+}$,yEu^{3+} phosphors show a regularly shift toward higher angle which may be due to the replacement of smaller Eu^{3+} ion ($r = 1.120$ Å, CN = 9) for La^{3+} ion ($r = 1.216$ Å, CN = 9) [17].

To further explore the crystal structure and confirm that the Tb^{3+} and Eu^{3+} ions are successfully introduced into the $NaLaMgWO_6$ host, the Rietveld refinement of three representative samples $NaLaMgWO_6$, $NaLa_{0.9}MgWO_6$:$0.1Tb^{3+}$, and $NaLa_{0.4}MgWO_6$:$0.1Tb^{3+}$,$0.5Eu^{3+}$ were performed by the Rietica software. According to the report on the structure evolution of $NaLaMgWO_6$ by Liu et al. [18], the un-doped $NaLaMgWO_6$ crystallizes in monoclinic structure with two possible space groups named *P*21 and *C*2/*m*, and the space group of *C*2/*m* has been proved to be more appropriate for the crystal structure of $NaLaMgWO_6$. Therefore, the space group *C*2/*m* was adopted as starting model for Rietveld refinement of above three samples, and the refined results are exhibited in Fig. 2. The red solid lines, crosses, blue bars, and green lines stand for calculated patterns, experimental data, Bragg positions, and differences between experimental data and calculated patterns, respectively. The refined R_p and R_{wp} for $NaLaMgWO_6$, $NaLa_{0.9}MgWO_6$:$0.1Tb^{3+}$ and $NaLa_{0.4}MgWO_6$:$0.1Tb^{3+}$,$0.5Eu^{3+}$ are 5.308/5.683/6.138 (R_p) and 7.109/8.929/9.677 (R_{wp}), respectively, which indicates that un-doped and doped NaLaMgWO6 samples are good agreement with the space group *C*2/*m*. Moreover, the refined unite cell parameters are displayed in Table 1. It is obvious that the lattice parameters (*a*, *b*, *c*) and unite cell volume (*V*) of $NaLa_{0.9}MgWO_6$:$0.1Tb^{3+}$ and $NaLa_{0.4}MgWO_6$:$0.1Tb^{3+}$, $0.5Eu^{3+}$ are smaller than those of un-doped NaLaMgWO6

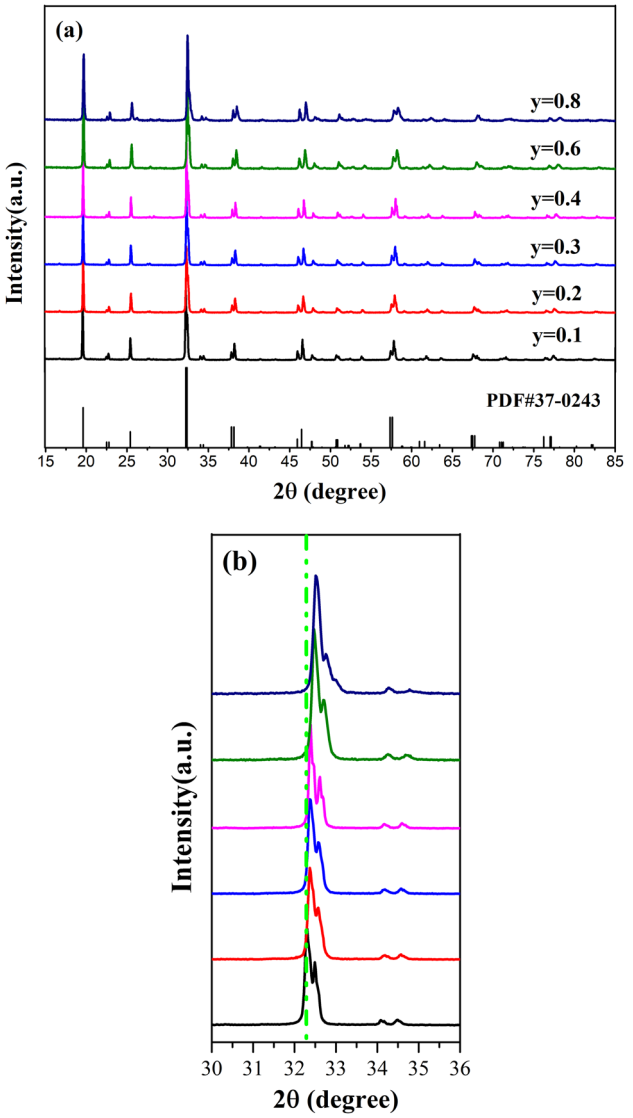

Fig. 1 **a** XRD patterns of $NaLa_{0.9-y}MgWO_6{:}0.1Tb^{3+}$, yEu^{3+} ($0.1 \le y \le 0.8$) phosphors; **b** the enlarged XRD patterns in the range of 30°–36°

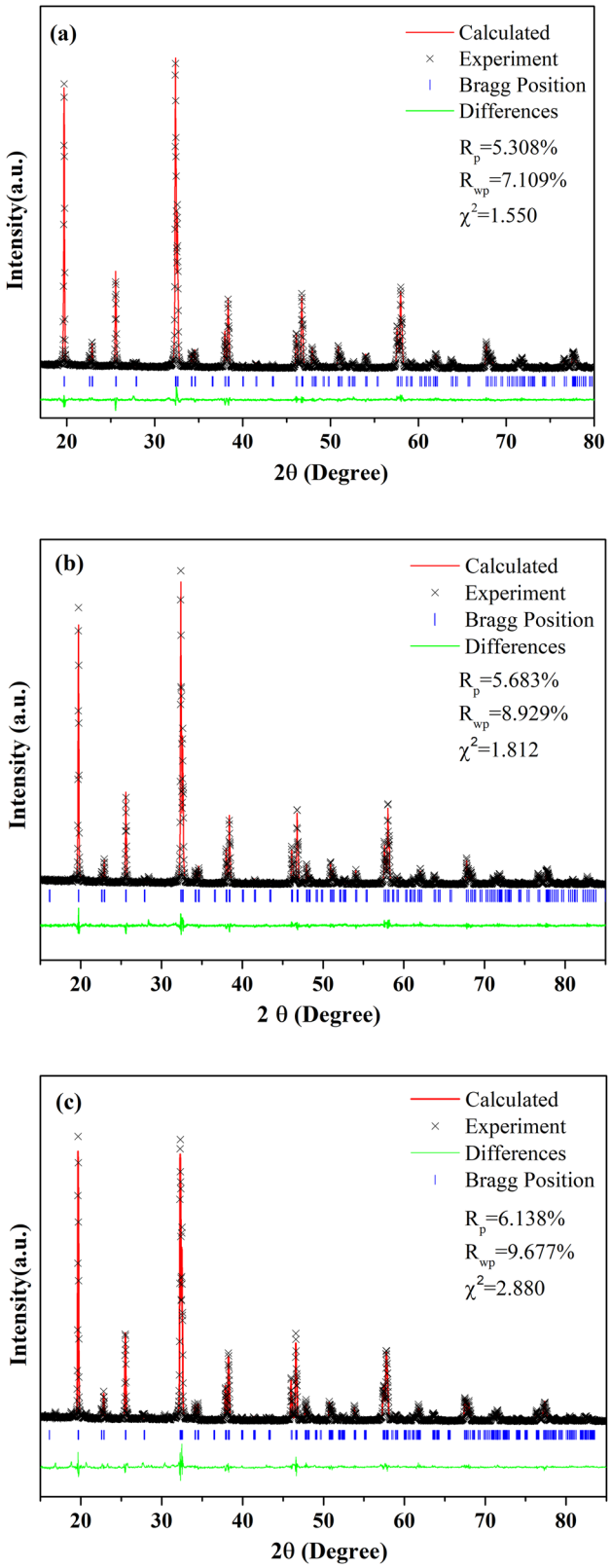

Fig. 2 Refined XRD patterns of **a** $NaLaMgWO_6$, **b** $NaLa_{0.9}MgWO_6{:}0.1Tb^{3+}$ and **c** $NaLa_{0.4}MgWO_6{:}0.1Tb^{3+}$, $0.5Eu^{3+}$ phosphors

host. The lattice shrinkage confirms further the successful substitution of smaller Tb^{3+}/Eu^{3+} ions for La^{3+} ions, and the substitution has no obvious effect on the structure of $NaLaMgWO_6$.

3.2 SEM and EDX study

In order to study the composition and element distribution of $NaLa_{0.4}MgWO_6{:}0.1Tb^{3+}$, $0.5Eu^{3+}$ phosphor, the elemental mapping and EDX spectrum are shown in Fig. 3. The sample contains spherical-like particles with good dispersion and uniform particle size. The particle size is in the range of 0.5–2 µm. In addition, EDX spectrum of the sample suggests that the sample is composed of Eu, Tb, Na, La,

Table 1 Crystallographic data for $NaLaMgWO_6$, $NaLa_{0.9}MgWO_6$:$0.1Tb^{3+}$ and $NaLa_{0.4}MgWO_6$:$0.1Tb^{3+}$,$0.5Eu^{3+}$ based on Rietveld refinement

Formula	$NaLaMgWO_6$	$NaLa_{0.9}MgWO_6$:$0.1Tb^{3+}$	$NaLa_{0.4}MgWO_6$:$0.1Tb^{3+}$,$0.5Eu^{3+}$
Crystal system	Monoclinic	Monoclinic	Monoclinic
Space group	*C*2/*m*	*C*2/*m*	*C*2/*m*
Lattice parameters			
a (Å)	7.7954	7.7878	7.7588
b (Å)	7.8008	7.7886	7.7643
c (Å)	7.893	7.8865	7.8675
$\alpha=\beta$ (°)	90	90	90
γ (°)	90.138	90.014	89.987
Cell volume (Å^3)	479.977	477.097	473.949
R-factors			
R_p %	5.308	5.683	6.138
R_{wp} %	7.109	8.929	9.677
χ^2	1.55	1.812	2.88

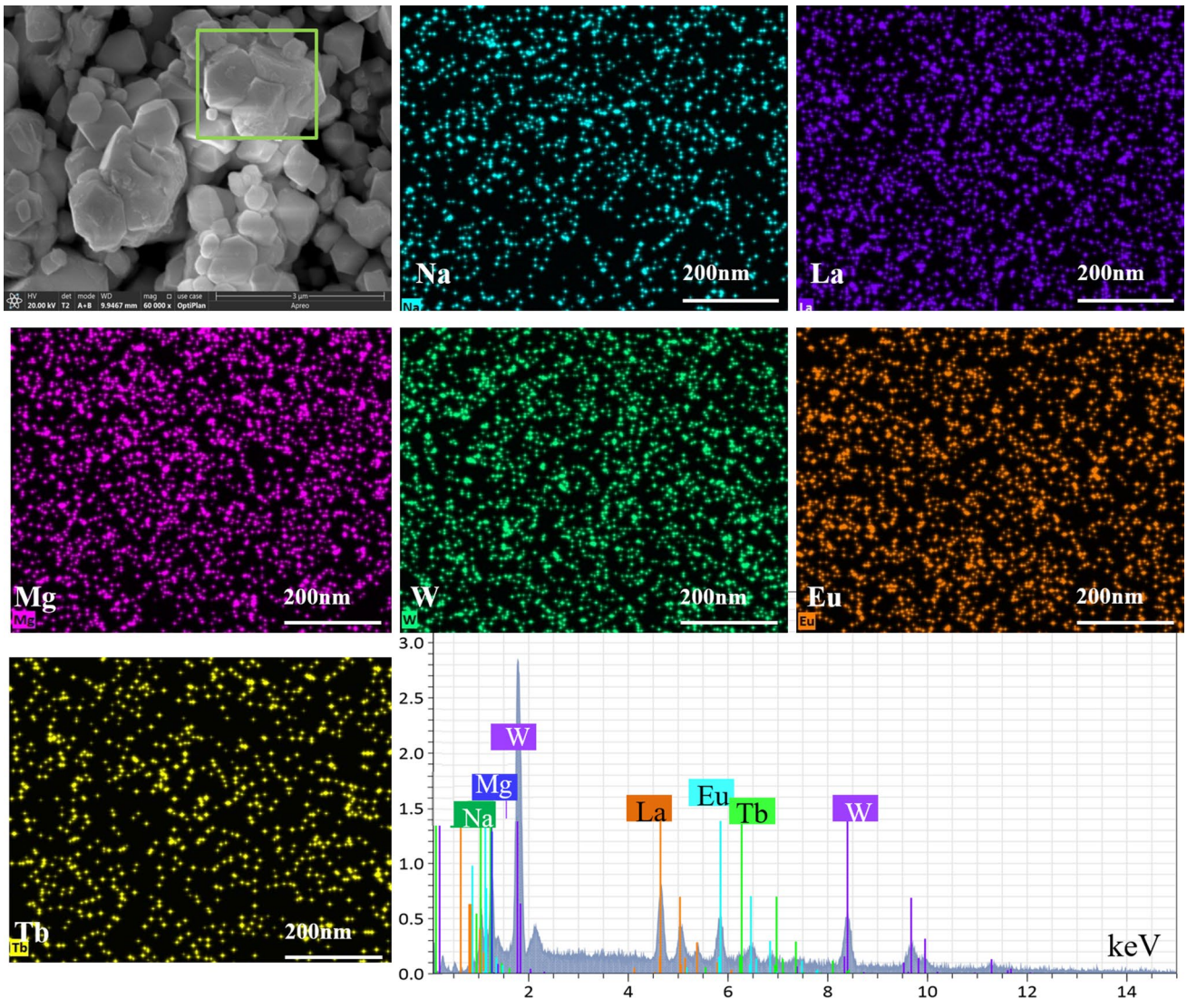

Fig. 3 SEM image, elemental mapping, and EDX spectrum of $NaLa_{0.4}MgWO_6$:$0.1Tb^{3+}$, $0.5Eu^{3+}$ phosphor

Mg, W, and O elements, and the elements of Tb, Eu, Na, La, Mg, and W are uniformly distributed throughout the whole particle. The results further manifest that Eu^{3+} and Tb^{3+} ions are incorporated into $NaLaMgWO_6$ host, and the $NaLaMgWO_6$:Tb^{3+},Eu^{3+} phosphor can be achieved.

3.3 Photoluminescence properties

Figure 4a displays the excitation and emission spectra of Tb^{3+} single-doped $NaLa_{0.9}MgWO_6$ phosphors by monitoring excitation and emission wavelength at 273 nm and 545 nm, respectively. The excitation spectrum contains a strong broad band ranging from 250 to 350 nm and a series of weak narrow peaks in the range of 350–450 nm. The broad band located at 273 nm is ascribed to the spin-forbidden and spin-allowed $4f^8 \rightarrow 4f^7 5d$ transitions of Tb^{3+} ions. The weak peaks are located at 357 nm, 368 nm, and 378 nm, corresponding to $^7F_6 \rightarrow {}^5D_2$, $^7F_6 \rightarrow {}^5L_{10}$, and $^7F_6 \rightarrow {}^5D_3$ transitions of Tb^{3+} ions, respectively [19, 20]. Under the excitation of 273 nm, The emission spectrum of $NaLa_{0.9}MgWO_6$:$0.1Tb^{3+}$ comprises of four emission peaks at 486 nm, 545 nm, 585 nm and 623 nm, which correspond to $^5D_4 \rightarrow {}^7F_6$, $^5D_4 \rightarrow {}^7F_5$, $^5D_4 \rightarrow {}^7F_4$, and $^5D_4 \rightarrow {}^7F_3$ transitions of Tb^{3+} ions, respectively [21]. Moreover, the emission intensity of $NaLa_{1-x}MgWO_6$:xTb^{3+} phosphors is related to Tb^{3+} doping concentration. As shown in Fig. 4b, with the increase of Tb^{3+} doping content, the emission intensity of $NaLa_{1-x}MgWO_6$:xTb^{3+} phosphor increases initially and reaches maximum at x = 0.1, then exhibit a decrement tendency due to the effect of concentration quenching.

The Fig. 5 demonstrates the excitation and emission spectra of Eu^{3+} single-doped $NaLaMgWO_6$ phosphors. The excitation spectrum of $NaLaMgWO_6$:Eu^{3+} (Fig. 5a) consists of a broad band located at 313 nm with several line peaks

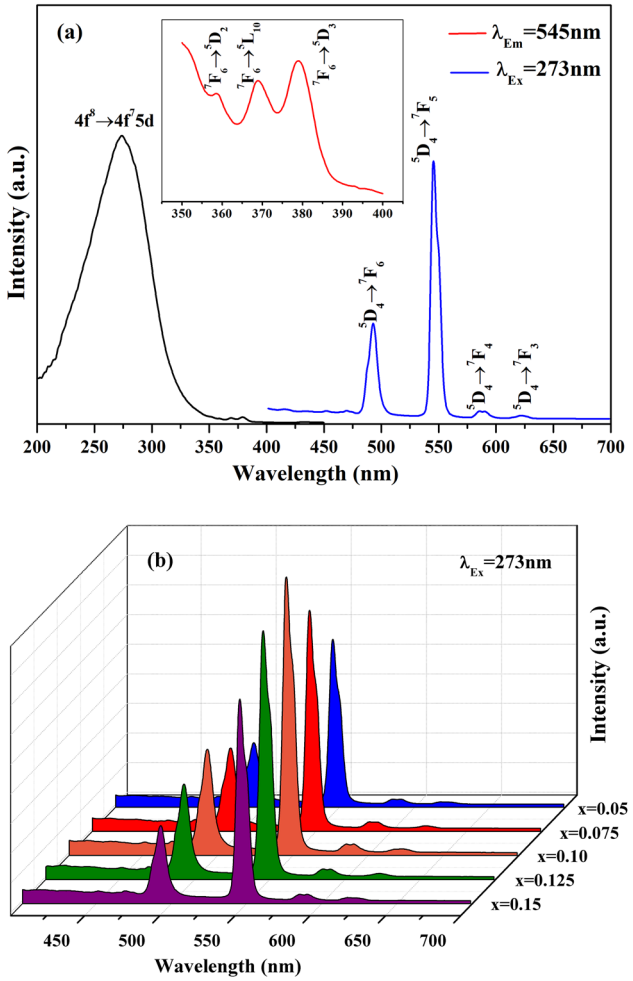

Fig. 4 **a** Excitation and emission spectra of $NaLa_{0.9}MgWO_6$:$0.1Tb^{3+}$ phosphors (λ_{Em} = 545 nm and λ_{Ex} = 273 nm). **b** Emission spectra of $NaLa_{1-x}MgWO_6$:xTb^{3+} (x = 0.05, 0.075, 0.1, 0.125, 0.15). The inset in (**a**) shows amplification of excitation spectrum in the range of 350–400 nm

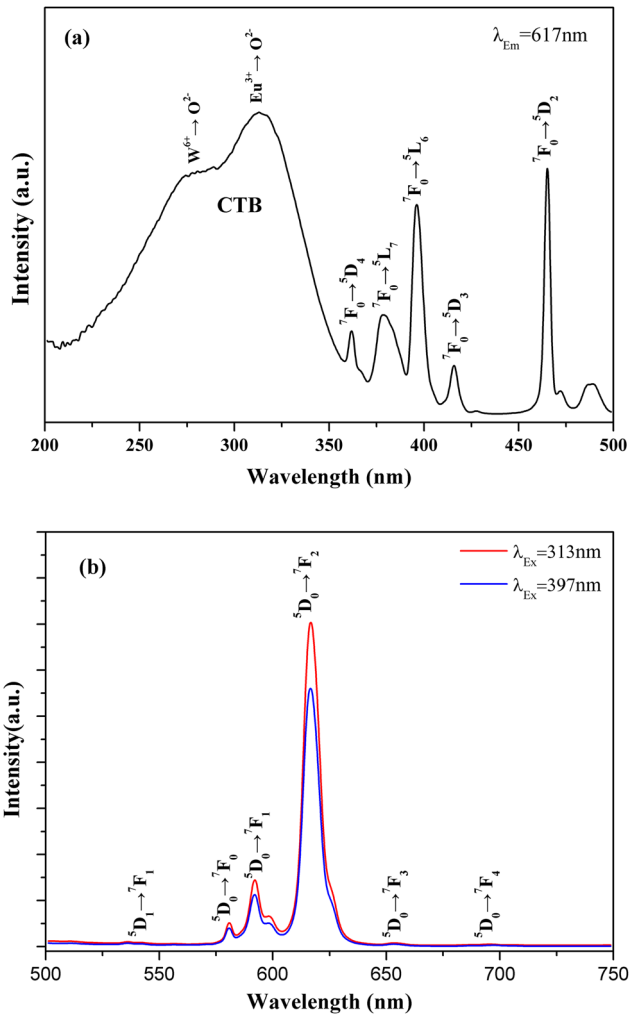

Fig. 5 **a** Excitation spectrum of $NaLaMgWO_6$: Eu^{3+} phosphors (λ_{em} = 617 nm). **b** Emission spectra of $NaLaMgWO_6$: Eu^{3+} phosphors (λ_{ex} = 313 nm and 397 nm)

covering from 350 to 500 nm. The former broad band is attributed to the charge transfer band (CTB) of $O^{2-} \rightarrow W^{6+}$ in WO_4^{2-} and the CTB of $O^{2-} \rightarrow Eu^{3+}$ transition. The latter narrow peaks are assigned to the typical 4-4f transitions of Eu^{3+}ions. Figure 5b presents the emission spectra of $NaLaMgWO_6$:Eu^{3+} phosphors under excitation at 313 nm and 397 nm. The emission spectra have similar emission profile, which show the Eu^{3+} 4–4f transition peaks centered at 536 nm ($^5D_1 \rightarrow {}^7F_1$), 580 nm ($^5D_0 \rightarrow {}^7F_0$), 592 nm ($^5D_0 \rightarrow {}^7F_1$), 617 nm ($^5D_0 \rightarrow {}^7F_2$), 653 nm ($^5D_0 \rightarrow {}^7F_3$), and 695 nm ($^5D_0 \rightarrow {}^7F_4$) [15, 16]. Furthermore, the intensity of electric dipole transition ($^5D_0 \rightarrow {}^7F_2$, 617 nm) is much higher than that of magnetic dipole transition ($^5D_0 \rightarrow {}^7F_1$, 592 nm) for both emission spectra, indicating that the Eu^{3+} ions are placed to the non-centrosymmetric lattice sites in this double perovskite $NaLaMgWO_6$.

Figure 6a presents the excitation of Eu^{3+} and the emission spectra of Tb^{3+}. It can be seen that only small spectral overlap in the range of 475–510 nm could be found. Energy transfer between Tb^{3+} to Eu^{3+} generally increase with the spectral overlap. However, some literatures [7, 8] have proved that the energy transfer from the Tb^{3+} to Eu^{3+} can

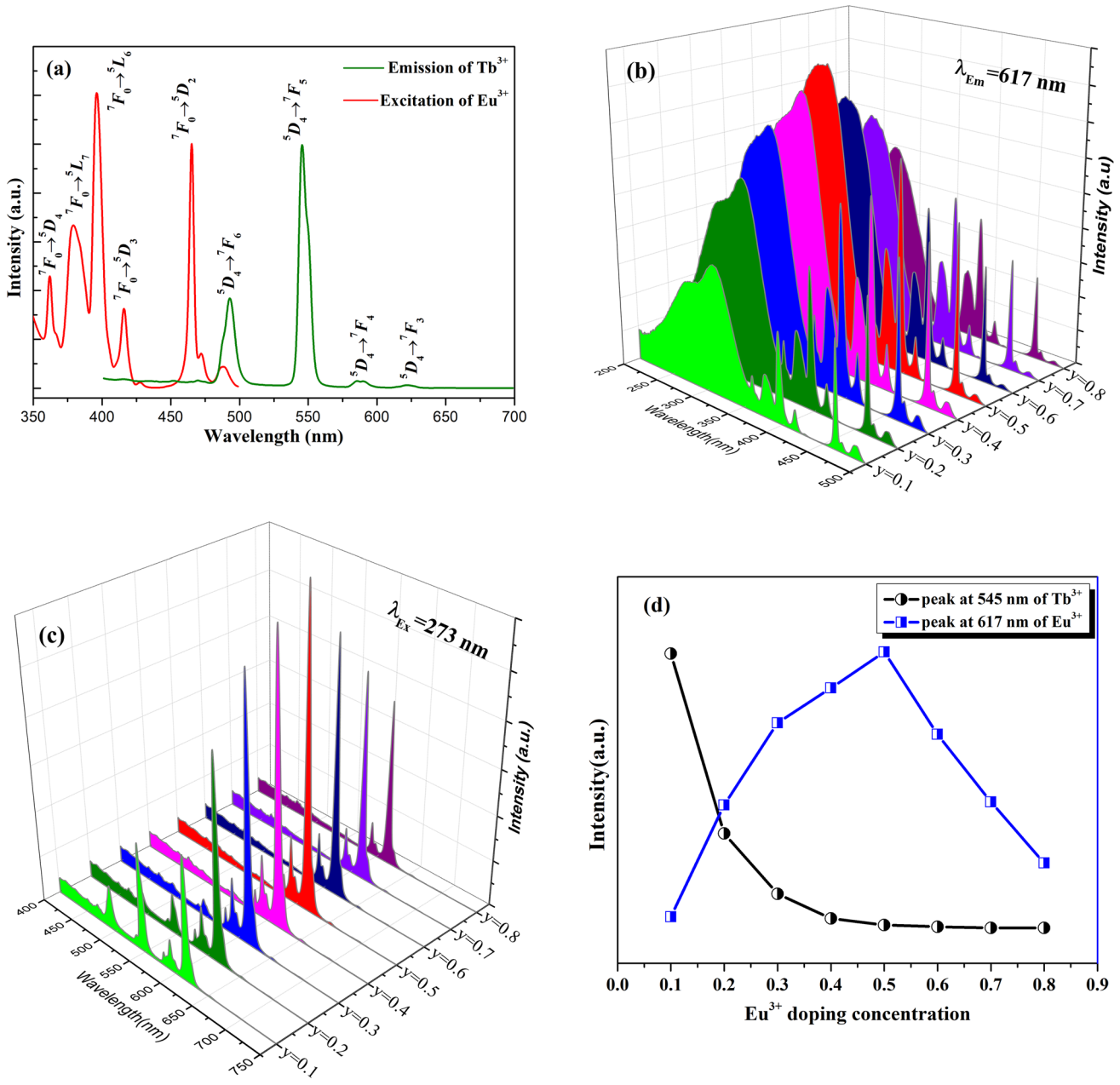

Fig. 6 **a** Excitation of Eu^{3+} and the emission spectra of Tb^{3+}; **b** excitation spectra of $NaLa_{0.9-y}MgWO_6$:$0.1Tb^{3+}$,yEu^{3+} phosphors; **c** emission spectra of $NaLa_{0.9-y}MgWO_6$:$0.1Tb^{3+}$,yEu^{3+} phosphors; **d** the relative emission intensity of Eu^{3+} ($^5D_0 \rightarrow {}^7F_2$) and Tb^{3+} ($^5D_4 \rightarrow {}^7F_5$) ($\lambda_{ex}$ = 273 nm)

still occur through assisted the phonons spectrum even if little spectral overlap. Figure 6b shows the excitation spectra of $NaLa_{0.9-y}MgWO_6$:0.1Tb^{3+},yEu^{3+} phosphors by monitoring with 617 nm. The excitation spectra are almost identical to that of $NaLaMgWO_6$: Eu^{3+} phosphors without any excitation peaks of Tb^{3+}. This is due to that the excitation peaks of Tb^{3+} overlap with those of Eu^{3+} and the spectrum intensity of Tb^{3+} is weaker than that of Eu^{3+}.

Figure 6c depicts the emission spectra of $NaLa_{0.9-y}MgWO_6$:0.1Tb^{3+},yEu^{3+} phosphors by exciting with 273 nm. At $y=0.1$, the emission spectrum of $NaLa_{0.8}MgWO_6$:0.1Tb^{3+},0.1Eu^{3+} phosphor contains both the typical $^5D_4 \rightarrow {}^7F_{6,5,4,3}$ transitions of Tb^{3+} ions and the $^5D_{0,1} \rightarrow {}^7F_{0,1,2,3,4}$ transitions of Eu^{3+} ions. In addition, with the increase of Eu^{3+} doping content, the emission intensity of Tb^{3+} decreases monotonically, while the intensity of Eu^{3+} increases initially then reduces, and its maximum is observed when $y=0.5$ (Fig. 6d). It demonstrates the presence of energy transfer from Tb^{3+} to Eu^{3+} and indicates that the color tuning of the emission from green to red could be realized by precisely changing the ratio of Eu^{3+}/Tb^{3+} ions concentration. The corresponding CIE chromaticity coordinates and CIE chromaticity diagram of $NaLa_{0.9-y}MgWO_6$:0.1Tb^{3+},yEu^{3+} phosphors are estimated and exhibited in Fig. 7. The emission color of $NaLa_{0.9}MgWO_6$:0.1Tb^{3+} phosphor is green with CIE coordinates of (0.293, 0.586) (Fig. 7a). With raising Eu^{3+} concentration, the emission hue changes from green (0.293, 0.586) to red (0.648, 0.351).

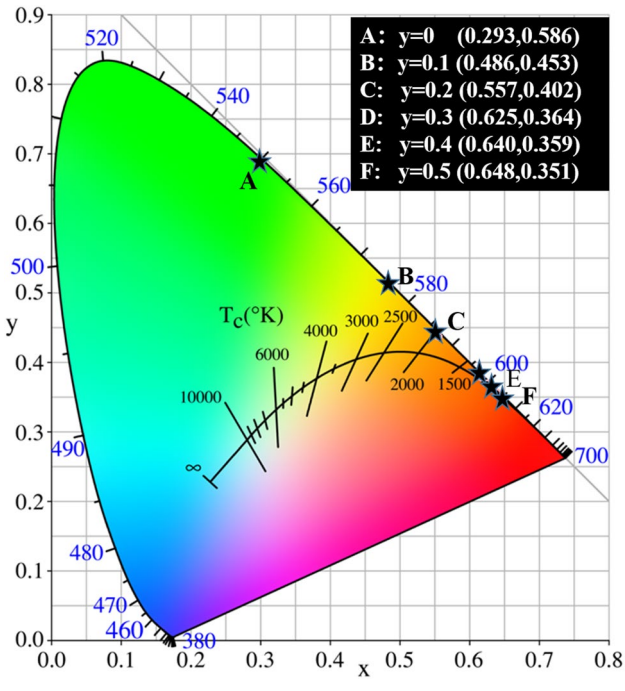

Fig. 7 CIE chromaticity coordinates for $NaLa_{0.9-y}MgWO_6$:0.1Tb^{3+},yEu^{3+} phosphors under 273 nm excitation

3.4 Decay curves and energy transfer mechanism

To explore the energy transfer process from Tb^{3+} to Eu^{3+}, the luminescence decay curves of $NaLa_{0.9-y}MgWO_6$:0.1Tb^{3+},yEu^{3+} phosphors excited at 273 nm and monitored at 545 nm are measured and presented in Fig. 8. It can be seen that the decay curves can be fitted with the following biexponential function:

$$I(t) = I_o + A_1 \exp\left(-t/\tau_1\right) + A_2 \exp\left(-t/\tau_2\right) \quad (1)$$

where I_0 and $I(t)$ represent the luminescence intensities at time t=0 and t, respectively. τ_1 and τ_2 refer to the decay lifetimes for the exponential components. A_1 and A_2 are the fitting coefficient. The average lifetime can be derived from the following equation [22]:

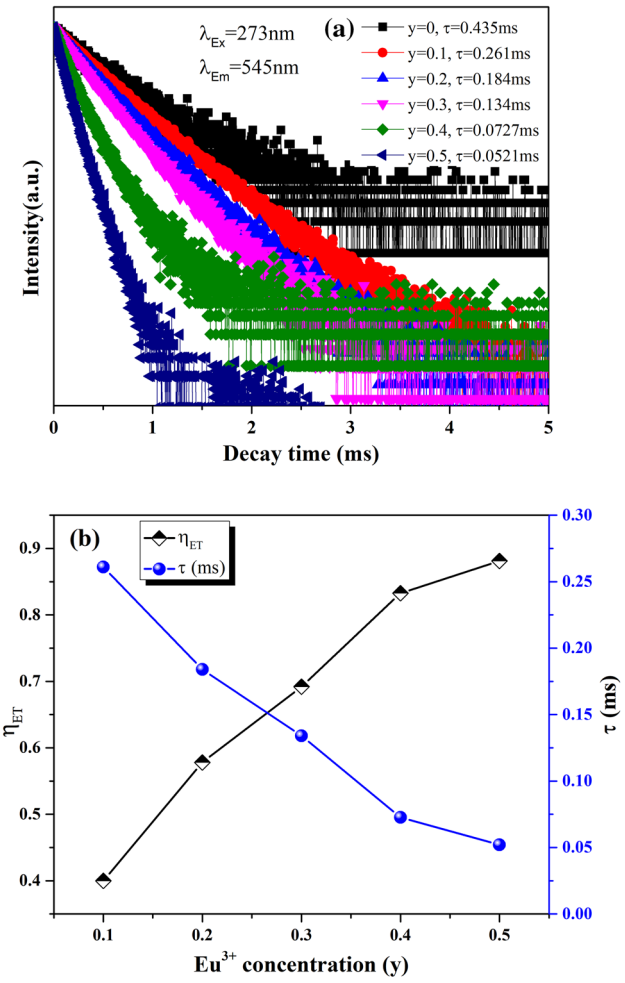

Fig. 8 **a** Luminescence decay curves of Tb^{3+} for $NaLa_{0.9-y}MgWO_6$:0.1Tb^{3+},yEu^{3+} phosphors; **b** the corresponding lifetime and energy transfer efficiency as a function of Eu^{3+} concentration

$$\tau = \left(A_1\tau_1^2 + A_2\tau_2^2\right)/\left(A_1\tau_1 + A_2\tau_2\right) \quad (2)$$

From the Eq. (2), the average decay lifetimes for $NaLa_{0.9-y}MgWO_6$:0.1Tb^{3+},yEu^{3+} phosphors are determined to be 0.435, 0.261, 0.184, 0.134, 0.0727, and 0.0521 ms for y = 0, 0.1, 0.2, 0.3, 0.4, and 0.5, respectively. In general, the decay lifetime of the sensitizer will be shorten due to the influence of energy transfer from the sensitizer to the activator. As shown in Fig. 8, the decay lifetime of Tb^{3+} decreases monotonically with the increase of Eu^{3+} doping concentration, which strongly indicates that Tb^{3+} ion can act as a good sensitizer, transferring its energy to activator Eu^{3+} in the $NaLa_{0.9-y}MgWO_6$:0.1Tb^{3+},yEu^{3+} phosphors. On the basis of the obtained decay lifetimes, the energy transfer efficiency (η_{ET}) from Tb^{3+} to Eu^{3+} can be determined by the following formula [6, 7]:

$$\eta_{ET} = 1 - \frac{\tau_s}{\tau_{s0}} \quad (3)$$

where τ_s and τ_{so} refer to the lifetimes of the sensitizer Tb^{3+} with and without the activator Eu^{3+}. According to the Eq. (3), the η_{ET} values of $NaLa_{0.9-y}MgWO_6$:0.1Tb^{3+},yEu^{3+} (y = 0, 0.1, 0.2, 0.3, 0.4, 0.5) phosphors are estimated and exhibited in Fig. 8b. The energy transfer efficiency η_{ET} increases with the increase of the Eu^{3+} content and reaches the maximum of 88.11% at y = 0.5, suggesting that the energy of Tb^{3+} can be efficiently transfer to Eu^{3+} in $NaLaMgWO_6$:Tb^{3+},Eu^{3+}phosphors.

General speaking, the energy transfer from sensitizers to activators in host is associated with exchange and multipolar interaction [23]. The prerequisite of exchange interaction mechanism is that the critical distance (R_c) between the sensitizer and activator is less than about 0.5 nm. As suggested by Blasse, the critical distance (R_c) between Tb^{3+} and Eu^{3+} in $NaLaMgWO_6$ host can be estimated using the following formula [24]:

$$R_C = 2\left(\frac{3V}{4\pi\chi_C N}\right)^{1/3} \quad (4)$$

where V is the volume of the unit cell, N is the number of the La^{3+} lattice sites in the unit cell, and χ_c is the total concentration of Tb^{3+} and Eu^{3+}. For $NaLa_{0.4}MgWO_6$:0.1Tb^{3+},0.5Eu^{3+} phosphors, V = 473.949 Å, N = 4, and χ_c = 0.6. Therefore, the critical distance (R_c) is estimated to be 7.23 Å. This value is longer than 5 Å for the exchange interaction, indicating the multipolar interaction play a leading role in the mechanism of energy transfer between Tb^{3+} and Eu^{3+}.

According to Dexter's energy transfer formula of multipolar interaction, the ratio of the luminescence quantum efficiency of the sensitizer in the absence of activation to the efficiency of the sensitizer in the presence of activation can be defined as [23, 25]:

$$\frac{\eta_0}{\eta} = C^{n/3} \quad (5)$$

where η_0 and η are the quantum efficiencies of Tb^{3+} without and with Eu^{3+}, respectively. C is the sum content of Tb^{3+} and Eu^{3+}, and n = 6, 8, 10, which correspond to dipole–dipole (d–d), dipole–quadrupole (d–q) and quadrupole–quadrupole (q–q) interaction, respectively. Experimentally, the value of η_0/η can be estimated approximately by the ratio of luminescence intensities (I_0/I) based on Reisfeld's approximation [3, 26]. Figure 9 shows the relationships of I_0/I versus $C^{n/3}$ for

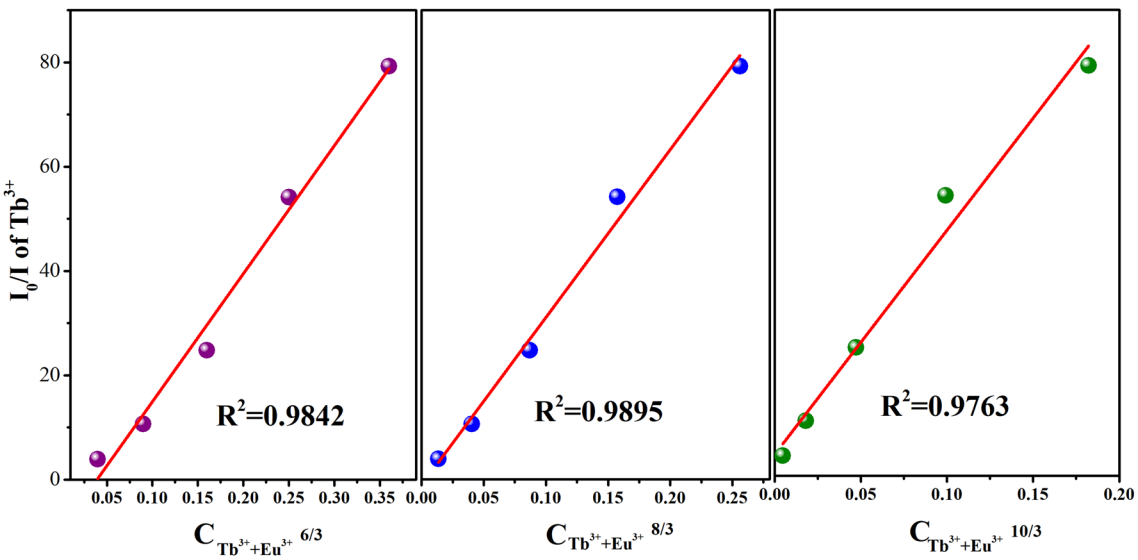

Fig. 9 Dependence of I_0/I of Tb^{3+} on $C_{Tb+Eu}^{n/3}$

$NaLaMgWO_6$:Tb^{3+},Eu^{3+} phosphors. It is obvious that the optimal linear relationship is observed when $n=8$, indicating that the energy transfer from Tb^{3+} to Eu^{3+} is realized via dipole–quadrupole interaction.

3.5 Thermal quenching properties

The thermal quenching temperature of the phosphors is a vital parameter for their practical application in high power white LEDs. The temperature-dependent emission spectra for $NaLa_{0.4}MgWO_6$:0.1Tb^{3+}, 0.5Eu^{3+} phosphors excited by 273 nm was measured and shown in Fig. 10a. The emission intensity declined gradually with the increase of the temperature, and the emission intensity at 455 K drops to 64.2% of the initial intensity at 305 K. It implies that

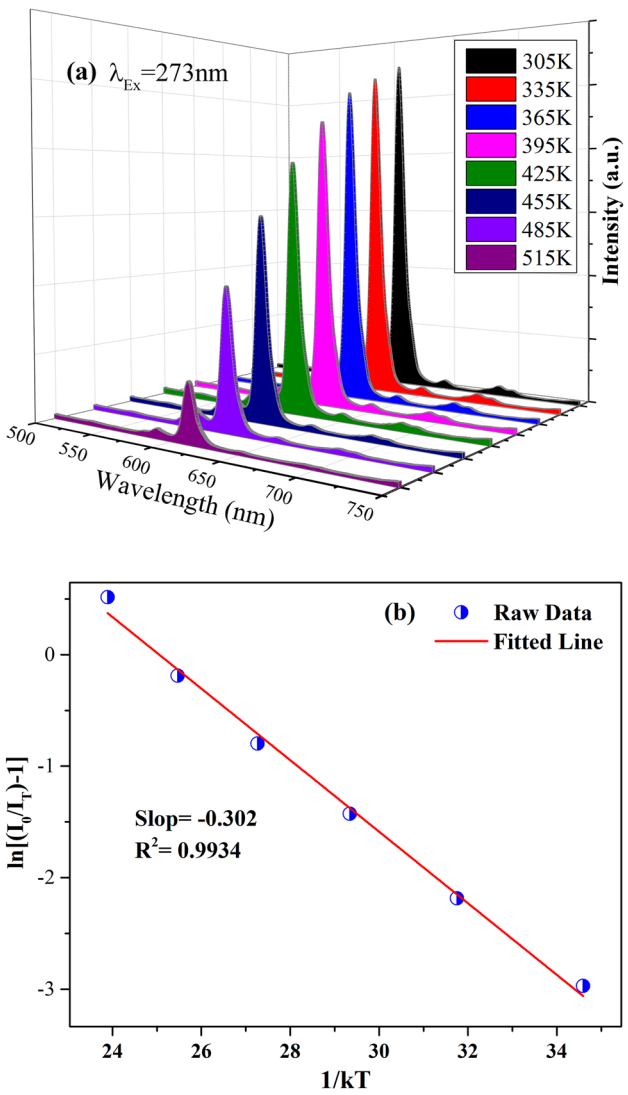

Fig. 10 **a** Emission spectra of $NaLa_{0.4}MgWO_6$:0.1Tb^{3+},0.5Eu^{3+} phosphors at different temperature ($\lambda_{ex}=273$ nm); **b** The plot of $\ln[(I_0/I_T) - 1]$ versus $1/kT$

$NaLa_{0.4}MgWO_6$:0.1Tb^{3+}, 0.5Eu^{3+} possesses excellent thermal stability. The thermal quenching is associated with the temperature of the electron–phonon interaction, affecting the ground state as well as the excited states [27]. The thermal quenching mechanism of $NaLa_{0.4}MgWO_6$:0.1Tb^{3+},0.5Eu^{3+} phosphors can be analyzed by calculating the activation energy according to the Arrhenius equation [5]:

$$I(T) = \frac{I_0}{1 + c\exp(-\Delta E/kT)} \tag{6}$$

where $I(T)$ and I_0 refer to the emission intensity at test temperatures and initial emission intensity, respectively. k is the Boltzmann constant (8.629×10^{-5} eV/K), c is the constant, and ΔE corresponds to the activation energy. The equation can be converted to the natural logarithm [28]:

$$\ln\left(\frac{I_0}{I_T} - 1\right) = -\frac{\Delta E}{kT} + c' \tag{7}$$

Figure 10b presents the plot of $\ln[(I_0/I_T) - 1]$ versus $1/kT$. The experimental data can be linear fitted with a slope of −0.302. Hence, based on the Arrhenius Eq. (7), the activation energy ΔE is approximately 0.302 eV for $NaLa_{0.4}MgWO_6$:0.1Tb^{3+}, 0.5Eu^{3+} phosphors.

4 Conclusions

In conclusion, Novel $NaLaMgWO_6$:Tb^{3+},Eu^{3+} phosphors with tunable emission color were successfully prepared by a solid-state reaction. X-ray diffraction study shows that $NaLaMgWO_6$:Tb^{3+},Eu^{3+} phosphors have the monoclinic crystal structure with the $C2/m$ space group, and Rietveld refinement demonstrates the effective replacement of La^{3+} by Tb^{3+} and Eu^{3+} in the host has no influence on the crystallinity of $NaLaMgWO_6$. Photoluminescence investigation reveals that with the increase of the ratio of Eu^{3+} to Tb^{3+}, the emission color of $NaLaMgWO_6$:Tb^{3+},Eu^{3+} phosphors can be tuned from green to red upon the excitation of ultraviolet light, and the corresponding CIE coordinates vary from (0.293, 0.586) to (0.648, 0.351). The energy transfer from Tb^{3+} to Eu^{3+} in $NaLaMgWO_6$ host is responsible for their tunable color emission, and the mechanism of energy transfer is confirmed to be the dipole–quadrupole interaction. Moreover, the thermal stability of $NaLaMgWO_6$:Tb^{3+},Eu^{3+} phosphors was also investigated and ΔE value is estimated to be 0.302 eV.

Acknowledgements This research was supported by the National Natural Science Foundation of Shaanxi Province (No. 2018JM5151)

References

1. D.D. Xu, W. Zhou, Z. Zhang, X.X. Ma, Z.G. Xia, Luminescence property and energy transfer behavior of apatite-type $Ca_4La_6(SiO_4)_4(PO_4)_2O_2$:$Tb^{3+}$, Eu^{3+}phosphor. Mater. Res. Bull. **108**, 101–105 (2018)
2. C. Liang, H.P. You, Y.B. Fu, X.M. Teng, K. Liu, J.H. He, Luminescence properties of a tunable blue-green-emitting $Ca_{10}(PO_4)_6S$:Ce^{3+}, T^{b3}+ phosphors for UV-excited white LEDs. Optik **131**, 335–342 (2017)
3. P.A.Nascimento, A.J. Silva, I.S. Carvalho, M.V. Rezende, Luminescence varied by selective excitation in Eu^{3+}, Tb^{3+}-doped $LiSrPO_4$ phosphors for W-LEDs applications, Opt. Mater. **96**, 109369 (2019)
4. Y.M. Feng, J.P. Huang, C.M. Li, G. Hu, J. Liu, X.B. Yu, Structure energy transfer and tunable photoluminescence of $Sr_7Zr(PO_4)_6$:Tb^{3+}, Eu^{3+} phosphors for near-UV white LEDs. J. Alloys Compd. **706**, 478–484 (2017)
5. B. Li, X.Y. Huang, H. Guo, Y.J. Zeng, Energy transfer and tunable photoluminescence of $LaBWO_6$:Tb^{3+}, E^{u3}+ phosphors for near-UV white LEDs. Dyes Pigments **150**, 67–72 (2018)
6. X.Y. Huang, B. Li, P. Du, H. Guo, R.P. Cao, J.S. Yu, K. Wang, Realizing highly efficient multicolor tunable emissions from Tb^{3+} and Eu^{3+} co-doped $CaGd_2(WO_4)_4$ phosphors via energy transfer by single ultraviolet excitation for lighting and display applications. Dyes Pigments **151**, 202–210 (2018)
7. M.J. Song, W. Zhao, W.G. Ran, J.P. Xue, Y.L. Liu, Multicolor tunable luminescence and energy transfer mechanism in a novel single-phase $KBaGd(WO_4)_3$:Tb^{3+}, E^{u3}+ phosphor for NUV. J. Alloys Compd. **803**, 1063–1074 (2019)
8. X. Zhang, J. Zhang, Y. Chen, M. Gong, Energy transfer and multicolor tunable emission in single-phase Tb3+, Eu^{3+} co-doped $Sr_3La(PO_4)^3$ phosphors. Ceram. Int. **42**, 13919–13924 (2016)
9. X.M. Zhu, Z.F. Zhou, Photoluminescence and energy transfer mechanism of a novel tunable color phosphor Na_2MgSiO_4:Tb^{3+}, Eu^{3+}. J. Lumin. **188**, 589–594 (2017)
10. Y.J. Liang, M.N. Hyeon, W.G. Ran, S.H. Park, C.C. Byung, J.H. Jeong, K.H. Kim, The design and synthesis of new double perovskite (Na, Li)YMg(W, $Mo_)O6$:^{Eu}3+ red phosphors for white light-emitting diodes. J. Alloys Compd. **716**, 56–64 (2017)
11. A.R. Sharits, J.F. Khoury, P.M. Woodward, Evaluating $NaREMgWO_6$ (RE=La, Gd, Y) doubly ordered double perovskites as Eu^{3+} Phosphor Hosts. Inorg. Chem. **55**, 12383–12390 (2016)
12. B. Han, Y.Z. Dai, J. Zhang, B.K. Liu, H.Z. Shi, Photoluminescence properties of a double perovskite tungstate based redemitting phosphor $NaLaMgWO_6$:Sm^{3+}. Ceram. Int. **44**, 3734–3740 (2018)
13. W.G. Ran, H.M. Noh, B.K. Moon, S.H. Park, J.H. Jeong, J.H. Kim, G.Z. Liu, J.S. Shi, Crystal structure, electronic structure and photoluminescence properties of $KLaMgWO_6$:Eu^{3+} phosphors. J. Lumin. **197**, 270–276 (2018)
14. L. Zhang, Z. Lu, P.D. Han, L.X. Wang, Q.T. Zhang, Synthesis and photoluminescence of Eu^{3+}-activated double perovskite $NaGdMg(W, Mo)_O6$: a potential red phosphor for solid state lighting. J. Mater. Chem. C **1**, 54–57 (2013)
15. L. Zhang, Q. Liu, N. Ding, H. Yang, L.X. Wang, Q.T. Zhang, Dual-channel enhanced luminescence of double perovskite $NaGdMgWO_6$:Eu^{3+} phosphor based on alternative excitation and delayed quenching. J. Alloys Compd. **642**, 45–52 (2015)
16. Q. Liu, L.X. Wang, L. Zhang, H. Yang, M.X. Yu, Q.T. Zhang, Enhanced luminescence and structure evolution of double perovskite (K, Na)$LaMgWO_6$:Eu^{3+} phosphor for white LEDs. J. Mater. Sci. **26**, 8083–8088 (2015)
17. R.D. Shannon, Revised effective ionic radii and systematic studies of interatomic distances in halides and chalcogenides. Acta. Crystallogr. A **32**, 751–767 (1976)
18. Q. Liu, X.B. Li, B. Zhang, L.X. Wang, Q.T. Zhang, L. Zhang, Structure evolution and delayed quenching of the double perovskite $NaLaMgWO_6$:Eu^{3+} phosphor for white LEDs. Ceram. Int. **42**, 15294–15300 (2016)
19. S. Chahar, R. Devi, M. Dalal, M. Bala, J. Dalal, P. Boora, V.B. Taxak, R. Lather, S.P. Khatkar, Color tunable nanocrystalline $SrGd_2Al_2O_7$:Tb^{3+} phosphor for solid state lighting. Ceram. Int. **45**, 606–613 (2019)
20. S.J. Park, B.S. Je, J.W. Jang, M.S. Oh, M.S. Koo, S.J. Yang, H.K. Yang, Green and red emitting YBO_3:Ln^{3+} (Ln=Eu, Tb) phosphors for detection of latent fingerprint. J. Alloys Compd. **789**, 367–374 (2019)
21. D.A. Hakeem, D.H. Kim, S.W. Kim, K. Park, Crystal structure and photoluminescence properties of novel garnet $Y_{2-x}LaCaGa_3ZrO_{12}$:xLn^{3+} (Ln = Eu and Tb) phosphors. Dyes Pigments **163**, 715–724 (2019)
22. J.X. Bin, H.K. Liu, L.F. Mei, L.M. Liang, H. Gao, H.S. Li, L.B. Liao, Multi-color luminescence evolution and efficient energy transfer of scheelite-type $LiCaGd(WO_4)_3$:Ln^{3+} (Ln = Eu, Dy, Tb) phosphors. Ceram. Int. **45**, 1837–1845 (2019)
23. L.G.Van Uitert, Characterization of energy transfer interactions between rare earth ions. J. Electrochem. Soc. **114**, 1048–1053 (1967)
24. D.L. Dexter, J.H. Schulman, Theory of concentration quenching in inorganic phosphors. J. Chem. Phys. **22**, 1063–1071 (1954)
25. D.L. Dexter, A theory of sensitized luminescence in solids. J. Chem. Phys. **12**, 2836–2850 (1953)
26. R. Reisfeld, N. Lieblich-Soffer, Energy transfer from UO_2^{2+} to Sm^{3+} in phosphate glass. J. Solid State Chem. **28**, 391–395 (1979)
27. X.B. Lia, Q. Liu, W.T. Huang, S.H. Chen, L.X. Wang, M.X. Yu, Q.T. Zhang, Structural and luminescent properties of Eu^{3+}-doped double perovskite $BaLaMgNbO_6$ phosphor. Ceram. Int. **44**, 1909–1915 (2018)
28. Q. Liu, L.X. Wang, W.T. Huang, L. Zhang, M.X. Yu, Q.T. Zhang, Enhanced luminescence properties of double perovskite (Ba, Sr) $LaMgSbO_6$:Eu^{3+} phosphors based on composition modulation. J. Alloys Compd. **717**, 156–163 (2017)